Ferromagnetism in CuFeSb: Evidence of competing magnetic interactions in iron-based superconductors

B. Qian, J. Lee, J. Hu, G. C. Wang, P. Kumar, M. H. Fang, T. J. Liu, D. Fobes, H. Pham, L. Spinu, X. S. Wu, M. Green, S. H. Lee, and Z. Q. Mao

Phys. Rev. B **85**, 144427 — Published 26 April 2012

DOI: 10.1103/PhysRevB.85.144427

Ferromagnetism in CuFeSb: Evidence of competing magnetic interactions in Fe-based superconductors

B. Qian[1,2,], J. Lee[3], J. Hu[1], G.C. Wang[1], P. Kumar[1], M. H. Fang[1], T. J. Liu[1], D. Fobes[1], H. Pham[4], L. Spinu[4], X. S. Wu[5], M. Green[6], S.H. Lee [3] and Z.Q. Mao[1*]

1. Department of Physics and Engineering Physics, Tulane University, New Orleans 70118 LA, USA

2. Advanced Functional Materials Lab and Department of Physics, Changshu Institute of Technology, Changshu 215500, China

3. Department of Physics, University of Virginia, Charlottesville, VA 22904, USA

4. Advanced Material Research Institute and Physics Department, University of New Orleans, LA 70148, USA

5. Laboratory of Solid State Microstructures and Department of Physics, Nanjing University, Nanjing 210093, China

6. NIST Center for Neutron Research, National Institute of Standards and Technology, 100 Bureau Drive, Gaithersburg, Maryland 20889, USA

Abstract

We have synthesized a new layered iron-pnictide CuFeSb. This material shares similar layered tetragonal structure with iron-based superconductors, with Fe square planar sheets forming from the edge-sharing iron antimony tetrahedral network. CuFeSb differs remarkably from Fe-based superconductors in the height of anion Z_{anion} from the Fe plane; Z_{Sb} for CuFeSb is ~1.84 Å, much larger than Z_{As} (1.31-1.51 Å) in FeAs compounds and Z_{Te} (~1.77 Å) in

$Fe_{1+y}Te$. In contrast with the metallic antiferromagnetic (AFM) or superconducting state of iron pnictides and chalcogenides under current studies, CuFeSb exhibits a metallic, ferromagnetic state with T_c = 375 K. This finding suggests that the competition between AFM and FM coupling may exist in Fe-based superconductors and that the nature of magnetic coupling within the Fe plane is indeed dependent on the height of anion as predicted in theories.

PACS numbers: 74.70.Xa, 75.10.-b, 75.30.Et

I. INTRODUCTION

Since the superconductivity in iron pnictides and chalcogenides occurs in close proximity to antiferromagnetically ordered states [1-8], the superconducting pairing mechanism has been suggested to be correlated to spin fluctuations [9-13]. The association of superconductivity with spin fluctuations is also manifested in the spin resonance of superconducting states [11-15]. In order to shed light on the essential role of spin fluctuations in superconducting pairing, enormous efforts have been devoted to study the mechanism of magnetism of undoped parent compounds as well as the interplay between magnetism and superconductivity in these materials. Although iron pnictides and chalcogenides share similar layered structure and Fermi-surface (FS) topology, the antiferromagnetic (AFM) orders of their undoped parent compounds are distinct: the pnictides such as LaOFeAs [16] and $BaFe_2As_2$ [17] show a "single-strip" AFM order with the in-plane wavevector being identical to the FS nesting wavevector (π,π), while the chalcogenide $Fe_{1+y}Te$ displays a "double-strip" AFM order with the in-plane wavevector of $(\pi,0)$ [18].

The distinct AFM structures between these two classes of materials have triggered intensive debate over the origin of magnetism. For iron pnictides, because the in-plane component of the AFM wavevector is identical to the FS nesting vector (π,π), its antiferromagnetism was considered to be driven by FS, *i.e.* spin-density wave (SDW) induced by FS nesting [19-23]. Nevertheless, this mechanism cannot be used to interpret the antiferromagnetism in $Fe_{1+y}Te$ since its in-plane component of the AFM wavevector is $(\pi,0)$, rather than the FS nesting vector (π,π). In addition to the picture of FS-driven magnetism, various models based on local moment superexchange interactions have been proposed [24-29] and a scenario of local moments coupled to a low number of itinerant electrons is also considered [24, 27, 30-31]. Moreover,

Yin *et al*. recently proposed an alternative unified microscopic model to interpret varying AFM correlations [32]. This model assumes coexistence of localized spins and itinerant electrons and that the AFM superexchange coupling between localized spins competes with the double-exchange ferromagnetic (FM) interaction by Hund's coupling between the localized spins and itinerant electrons. Both "single-strip" and "double-strip" AFM orders can be well understood in light of different height of anion Z_{anion} from the Fe plane between pnictide parent compounds and $Fe_{1+y}Te$.

The important role of the anion height in determining a magnetic ground state is also demonstrated in the first-principles calculations by Moon and Choi [33]. Their work showed that the magnetic state of $Fe_{1+y}Te$ would switch from the "double-strip" to the "single-strip" AFM order if the height of Te, Z_{Te}, was lowered below a critical value (~1.71 Å). This is consistent with the experimental observation that in $Fe_{1+y}(Te_{1-x}Se_x)$ the $(\pi,0)$ magnetic correlation gradually weakens as the increase of Se content reduces $Z_{Te/Se}$, but the (π,π) magnetic correlation enhances accordingly [7]. Furthermore, from the total energy calculation (Fig. 2a in ref. [33]), there appears to be a trend toward FM state with an increase of Z_{anion}. However, as far as we know, no ferromagnetism has been reported thus far in any iron pnictides/chalcogenides isostructural to ferrous superconductors. Here we report metallic ferromagnetism discovered in CuFeSb which shares similar layered tetragonal structure with Fe-based superconductors. The height of Sb from the Fe plane Z_{Sb} in this compound is ~1.84 Å, much larger than Z_{As} (1.31-1.51 Å) in FeAs compounds [16-17, 34] and Z_{Te} (~1.77 Å) in $Fe_{1+y}Te$ [18]. This result is in a good agreement with the theoretical result stated above.

II. EXPERIMENT

Polycrystalline samples of CuFeSb were synthesized using a solid state reaction method. The thoroughly mixed powder of Cu, Fe and Sb with the ratio of 1:1:1 was first pressed into pellets, then sealed in an evacuated quartz tube and sintered at 700 °C for 24 h. The samples were then reground, pressed into pellets, and sintered again at 700 °C for 24 h to ensure homogeneity. Structural characterization of the sample was performed using X-ray diffraction and neutron scattering. Neutron scattering data were collected on a powder sample with the weight of 18 g using high resolution powder diffractometer BT1 at the NIST Center for Neutron Research (NCNR), with Ge(311) monochromators giving wavelength 2.07820 Å and collimation of 15 minutes. The crystal and magnetic structures of the sample were refined using FullProf [35]. The sample composition was analyzed using energy dispersive x-ray spectrometer (EDXS). The magnetization measurements on the sample were performed using a Quantum Design SQUID magnetometer. The resistivity was measured using a standard four probe method in a Physical Property Measurement System (PPMS, Quantum Design).

III. RESULTS AND DISCUSSIONS

Both X-ray diffraction and neutron scattering analyses show that the CuFeSb sample crystallizes in the Cu_2Sb-type tetragonal structure with the space group $P4/nmm$. Figure 1 presents the neutron diffraction data collected at 400K and 20K, as well as the results of structural refinement. The refined structure is schematically displayed in Fig. 2. In addition to CuFeSb, we observed two minor phases FeSb and Fe_3O_4, with their contents being estimated to be ~ 2.63(1)% and 0.74(1)% respectively. FeSb is antiferromagntic with the NiAs structure [36], while Fe_3O_4 is a well-known ferrimagnet with T_c = 840 K. The lattice parameters of CuFeSb

derived from the refinement for 400 K are a = 3.93466(2) Å and c = 6.25152(4) Å. Other refined structural parameters, including atomic coordinates, bonding lengths and angles are summarized in Table 1. Neutron scattering measurements conducted at low temperatures reveal that CuFeSb does not undergo any structural transition. The composition analyses by EDXS confirm that the sample composition is indeed stoichiometric.

The crystal structure of CuFeSb is basically analogous to those of Fe-based superconductors, with particular similarity to LiFeAs [37]. Fe and Sb form anti-PbO-type layers, with Fe square planar sheets forming from the edge-sharing iron antimony tetrahedral network. This structural characteristic is exactly the same as the anti-PbO-type FeAs layers in pnictides or Fe(Te/Se) layers in chalcogenides. Cu ions occupy interstitial sites of Sb layers. In the FeSb layers, Sb ions form a distorted tetrahedral arrangement around Fe ions, giving rise to two distinct Sb−Fe−Sb bonding angles which are indicated by α and β in Fig. 2. α represents the Sb−Fe−Sb bonding angle formed by two neighboring Sb ions lying above the Fe plane, and β refers to the Sb−Fe−Sb angle formed by one Sb ion lying above and one Sb ion lying below the Fe plane (see Fig. 2). α and β are 93.860(5)° and 117.797(3)° respectively for CuFeSb, remarkably different from those for LiFeAs where α = 102.793(6)° and β = 112.910(3)° respectively [34]. Aside from the bonding angle difference, the Fe-Sb bonding length (2.693 Å) is appreciably greater than the Fe-As bonding length (2.4162(1) Å). These differences of bonding angles and lengths lead the height of Sb, Z_{Sb}, from the Fe plane to be strikingly larger than Z_{As} in FeAs compounds or Z_{Te} in $Fe_{1+y}Te$: Z_{Sb} is 1.84 Å for CuFeSb, while Z_{As} (Z_{Te}) is 1.51 Å for LiFeAs [34], 1.31 Å for LaOFeAs [16], 1.35 Å for $BaFe_2As_2$ [17] and 1.77 Å for $Fe_{1+y}Te$ [18].

Although CuFeSb shares similar tetragonal structure with the iron pnictides and chalcogenides under current studies, it exhibits ferromagnetism, in sharp contrast with the antiferromagnetism and superconductivity observed in current iron pnictides and chalcogenides. The ferromagnetism of CuFeSb is demonstrated in both magnetization and neutron scattering measurements. Figure 3a shows the magnetization M as a function of temperature for CuFeSb. A remarkable ferromagnetic transition is observed; the transition temperature is estimated to be 375 K from the derivative dM/dT. Typical irreversible behavior for a FM state was observed in $M(T)$ measured with zero-field-cooling (ZFC) and field-cooling (FC) histories. Figure 3b displays the magnetization vs. magnetic field $M(H)$ curves at 2 K and 100 K. At both temperatures, the magnetization saturates at very low field, indicating small magneto-crystalline anisotropy in this compound. Saturation moments are 1.70 and 1.62 μ_B/Fe at 2 and 100 K, respectively. These values are comparable to those theoretically calculated for LaFeAsO and $BaFe_2As_2$ compounds [20, 38]. As seen in the magnetic hysteresis loop at 2 K given in the right inset of Fig. 3b, the coercive force for this FM compound is rather small, indicating that CuFeSb is a soft ferromagnetic material. The temperature dependence of resistivity of this compound shows metallic behavior, as shown in the left inset of Fig. 3b.

In neutron scattering measurements, as the temperature is decreased below T_c, we observed the increase of the magnetic Bragg intensities on top of the nuclear Bragg peaks, as shown in the inset of Fig. 4 where the (001) diffraction peaks at various temperatures are presented. This implies the magnetic propagation vector Q_m=0. The magnetic Bragg peaks can be best fit with the ferromagnetic spin alignment on the Fe plane. Figure 1b shows the result of refinement for 20 K as an example. The exact direction of the spin on the plane is indistinguishable in the case of powder measurements, and for the refinements, it was arbitrarily

set to be parallel to the *a*-axis. This magnetic configuration is illustrated in Fig. 2. The variation of ordered magnetic moment with temperature is shown in the main panel of Fig. 4. The ordered magnetic moment starts to increase below the critical temperature, and becomes saturated around 1.5 μ_B/Fe below 200K, comparable to the saturated moment measured in the magnetization (see Fig. 3b). Moreover, from neutron scattering measurements, there appears to be a slight upturn of the magnetic moment at low temperature. However, given that the resolution of the refined magnetic moment is limited and we have only one data point below 100 K, further investigation is needed to clarify this increase of moment.

What is the origin of the metallic ferromagnetism in CuFeSb? The answer to this question would certainly be instrumental to the clarification of the magnetism mechanism of Fe-based superconductor parent compounds. From the discussions presented above, the large height of Sb from the Fe plane appears to play an important role in achieving ferromagnetism in CuFeSb. The larger Z_{Sb} would cause the coupling between the Fe t_{2g} states and the Sb 5p states to become weak and thus increase the density of state at the Fermi level, $N(E_F)$, according to the first principles calculation [33]. High $N(E_F)$ can explain metallic ferromagnetism in terms of Stoner criterion. The trend toward ferromagnetism for $Z_{anion} > 1.82$ Å has indeed been revealed in the DFT calculations for iron telluride [33]. Given $Z_{Sb} = 1.84$ Å for CuFeSb, our observation of metallic ferromagnetism fits fairly well with this theoretical result.

In addition, the ferromagnetism of CuFeSb can also be interpreted using the above-mentioned unified microscopic model proposed by Yin *et al.* [32]. The essential idea of this model is that in iron pnictides/chalcogenides there exists the competition between the AFM superexchange interaction of localized spins and the FM double-exchange interaction mediated

by the Hund's rule coupling between localized spins and itinerant electrons. Z_{anion} is a key parameter in tuning the relative strength of these two magnetic interactions. Large Z_{anion} weakens the AFM coupling, but enhances FM correlation. This can be easily understood given that the AFM superexchange interaction between localized spins at Fe sites occurs via the anions. When the anions are farther away from the Fe plane, the Fe-Fe superexchange interaction through the anions is naturally expected to become weak. With this idea in mind, the absence of antiferromagnetism in CuFeSb can be viewed as a natural consequence of the large Z_{Sb}. While we cannot exclude the possibility that the ferromagnetism of CuFeSb arises from Stoner instability, the double-exchange FM interaction is a reasonable alternative interpretation. Further investigation, including the first-principles calculation, is needed to elucidate this issue.

IV. CONCLUSIONS

In summary, we have synthesized a new material CuFeSb, which crystalizes in layered tetragonal structure similar to those of Fe-based superconductors. We observed metallic ferromagnetism in this compound, in sharp contrast with the antiferromagnetism and superconductivity observed in other iron pnictides and chalcogenides. Our analyses suggest that the large height of Sb from the Fe plane may play an important role in stabilizing a FM state in CuFeSb. Our findings support the theoretical idea that the anion height controls the competing magnetic interactions in Fe-based superconductors.

ACKNOWLEDGMENTS

We would like to acknowledge useful discussions with W. Ku, J.P. Hu, Z. Lu and D. Singh. Work at Tulane is supported by the NSF under grant DMR-0645305 and the LA-SiGMA program under Award No. EPS-1003897 -1-0031. Work at UV and NCNR were partly supported by the US Department of Energy through the contract DE-FG02-10ER46384. Work at NJU is supported by National Key Projects for Basic Research of China (No.2010CB923404). Work at CIT is supported by Qing Lan Project and NNSFC under Grant Nos. 11174043 and 10874021.

*Corresponding author: zmao@tulane.edu

REFERENCES

[1] J. Zhao, Q. Huang, C. de la Cruz, S. Li, J. W. Lynn, Y. Chen, M. A. Green, G. F. Chen, G. Li, Z. Li, J. L. Luo, N. L. Wang, and P. Dai, Nat. Mater. **7**, 953 (2008).

[2] H. Luetkens, H. H. Klauss, M. Kraken, F. J. Litterst, T. Dellmann, R. Klingeler, C. Hess, R. Khasanov, A. Amato, C. Baines, M. Kosmala, O. J. Schumann, M. Braden, J. Hamann-Borrero, N. Leps, A. Kondrat, G. Behr, J. Werner, and B. Buchner, Nat. Mater. **8**, 305 (2009).

[3] A. J. Drew, C. Niedermayer, P. J. Baker, F. L. Pratt, S. J. Blundell, T. Lancaster, R. H. Liu, G. Wu, X. H. Chen, I. Watanabe, V. K. Malik, A. Dubroka, M. Rossle, K. W. Kim, C. Baines, and C. Bernhard, Nat. Mater. **8**, 310 (2009).

[4] H. Chen, Y. Ren, Y. Qiu, W. Bao, R. H. Liu, G. Wu, T. Wu, Y. L. Xie, X. F. Wang, Q. Huang, and X. H. Chen, Europhys. Lett. **85**, 17006 (2009).

[5] J.-H. Chu, J. G. Analytis, C. Kucharczyk, and I. R. Fisher, Phys. Rev. B **79**, 014506 (2009).

[6] S. Nandi, M. G. Kim, A. Kreyssig, R. M. Fernandes, D. K. Pratt, A. Thaler, N. Ni, S. L. Bud'ko, P. C. Canfield, J. Schmalian, R. J. McQueeney, and A. I. Goldman, Phys. Rev. Lett **104**, 057006 (2010).

[7] T. J. Liu, J. Hu, B. Qian, D. Fobes, Z. Q. Mao, W. Bao, M. Reehuis, S. A. J. Kimber, K. Prokeš, S. Matas, D. N. Argyriou, A. Hiess, A. Rotaru, H. Pham, L. Spinu, Y. Qiu, V. Thampy, A. T. Savici, J. A. Rodriguez, and C. Broholm, Nat. Mater. **9**, 718 (2010).

[8] N. Katayama, S. Ji, D. Louca, S. Lee, M. Fujita, T. J. Sato, J. Wen, Z. Xu, G. Gu, G. Xu, Z. Lin, M. Enoki, S. Chang, K. Yamada, and J. M. Tranquada, J. Phys. Soc. Jpn. **79** (2010).

[9] K. Ahilan, F. L. Ning, T. Imai, A. S. Sefat, R. Jin, M. A. McGuire, B. C. Sales, and D. Mandrus, Phys. Rev. B **78**, 100501 (2008).

[10] Y. Nakai, K. Ishida, Y. Kamihara, M. Hirano, and H. Hosono, J. Phys. Soc. Jpn. **77**, 073701 (2008).

[11] A. D. Christianson, E. A. Goremychkin, R. Osborn, S. Rosenkranz, M. D. Lumsden, C. D. Malliakas, I. S. Todorov, H. Claus, D. Y. Chung, M. G. Kanatzidis, R. I. Bewley, and T. Guidi, Nature **456**, 930 (2008).

[12] M. D. Lumsden, A. D. Christianson, D. Parshall, M. B. Stone, S. E. Nagler, G. J. MacDougall, H. A. Mook, K. Lokshin, T. Egami, D. L. Abernathy, E. A. Goremychkin, R. Osborn, M. A. McGuire, A. S. Sefat, R. Jin, B. C. Sales, and D. Mandrus, Phys. Rev. Lett **102**, 107005 (2009).

[13] S. Chi, A. Schneidewind, J. Zhao, L. W. Harriger, L. Li, Y. Luo, G. Cao, Z. a. Xu, M. Loewenhaupt, J. Hu, and P. Dai, Phys. Rev. Lett **102**, 107006 (2009).

[14] H. A. Mook, M. D. Lumsden, A. D. Christianson, B. C. Sales, R. Jin, M. A. McGuire, A. Sefat, D. Mandrus, S. E. Nagler, and T. Egami, arXiv:0904.2178 (2009).

[15] Y. Qiu, W. Bao, Y. Zhao, C. Broholm, V. Stanev, Z. Tesanovic, Y. C. Gasparovic, S. Chang, J. Hu, B. Qian, M. Fang, and Z. Mao, Phys. Rev. Lett **103**, 067008 (2009).

[16] C. de la Cruz, Q. Huang, J. W. Lynn, J. Li, W. R. Ii, J. L. Zarestky, H. A. Mook, G. F. Chen, J. L. Luo, N. L. Wang, and P. Dai, Nature **453**, 899 (2008).

[17] Q. Huang, Y. Qiu, W. Bao, M. A. Green, J. W. Lynn, Y. C. Gasparovic, T. Wu, G. Wu, and X. H. Chen, Phys. Rev. Lett **101**, 257003 (2008).

[18] W. Bao, Y. Qiu, Q. Huang, M. A. Green, P. Zajdel, M. R. Fitzsimmons, M. Zhernenkov, S. Chang, M. Fang, B. Qian, E. K. Vehstedt, J. Yang, H. M. Pham, L. Spinu, and Z. Q. Mao, Phys. Rev. Lett **102**, 247001 (2009).

[19] J. Dong, H. J. Zhang, G. Xu, Z. Li, G. Li, W. Z. Hu, D. Wu, G. F. Chen, X. Dai, J. L. Luo, Z. Fang, and N. L. Wang, Europhys. Lett. **83**, 27006 (2008).

[20] D. J. Singh, Phys. Rev. B **78**, 094511 (2008).

[21] F. Ma, and Z.-Y. Lu, Phys. Rev. B **78**, 033111 (2008).

[22] V. Cvetkovic, and Z. Tesanovic, Europhys. Lett. **85**, 37002 (2009).

[23] I. I. Mazin, Nature **464**, 183 (2010).

[24] F. Ma, Z.-Y. Lu, and T. Xiang, Phys. Rev. B **78**, 224517 (2008).

[25] Q. Si, and E. Abrahams, Phys. Rev. Lett **101**, 076401 (2008).

[26] T. Yildirim, Phys. Rev. Lett **101**, 057010 (2008).

[27] F. Ma, W. Ji, J. Hu, Z.-Y. Lu, and T. Xiang, Phys. Rev. Lett **102**, 177003 (2009).

[28] J. Hu, B. Xu, W. Liu, N.-N. Hao, and Y. Wang, arXiv: 1106.5169 (2011).

[29] J. Hu, and H. Ding, arXiv: 1107.1334 (2011).

[30] J. Wu, P. Phillips, and A. H. C. Neto, Phys. Rev. Lett **101**, 126401 (2008).

[31] M. D. Johannes, and I. I. Mazin, Phys. Rev. B **79**, 220510 (2009).

[32] W.-G. Yin, C.-C. Lee, and W. Ku, Phys. Rev. Lett **105**, 107004 (2010).

[33] C.-Y. Moon, and H. J. Choi, Phys. Rev. Lett **104**, 057003 (2010).

[34] M. J. Pitcher, D. R. Parker, P. Adamson, S. J. C. Herkelrath, A. T. Boothroyd, R. M. Ibberson, M. Brunelli, and S. J. Clarke, Chem. Commun., 5918 (2008).

[35] J. Rodríguez-Carvajal, Physica B **192**, 55 (1993).

[36] K. Yamaguchi, H. Yamamoto, Y. Yamaguchi, and H. Watanabe, J. Phys. Soc. Jpn. **33**, 1292 (1972).

[37] X. C. Wang, Q. Q. Liu, Y. X. Lv, W. B. Gao, L. X. Yang, R. C. Yu, F. Y. Li, and C. Q. Jin, Solid State Commun. **148**, 538 (2008).

[38] I. I. Mazin, and M. D. Johannes, Nat. Phys. **5**, 141 (2009).

Table 1: Refined structure parameters for CuFeSb at 400 K. The number in square brackets indicates the number of symmetry of equivalent bond lengths.

Space group *P*4/*nmm* , $a = b = 3.93466(2)$ Å, $c = 6.25152(4)$ Å

		x	***y***	***z***	***B* (Å^2)**	**Wyckoff positions**
Atomic coordinates	**Cu**	0.25	0.25	0.71967(42)	1.028(48)	2c
	Fe	0.75	0.25	0	1.184(28)	2b
	Sb	0.25	0.25	0.29418(53)	0.950(68)	2c

	Fe-Sb [4]	**Fe-Fe [4]**	**Cu-Sb [1]**	**Cu-Sb [4]**
Bond lengths (Å)	2.693(1)	2.782(2)	2.660(3)	2.784(2)

Bond angles (°) **Sb-Fe-Sb**	α =93.860(5)	β =117.797(3)

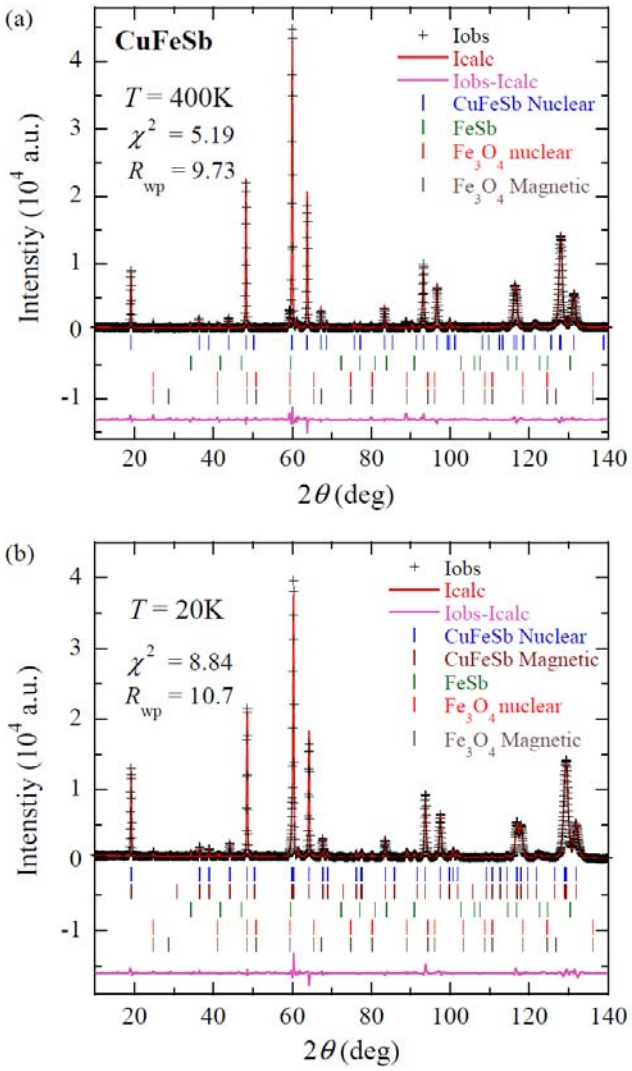

Figure 1(Color online). Neutron powder diffraction spectra (+) of CuFeSb and the results of FullProf. refinements (solid line) at 400 K (a) and 20 K (b). The difference between the experimental data and the fitting line is shown at the bottom in both (a) and (b). Tick marks indicate nuclear Bragg diffraction peak positions of CuFeSb/minor impurity phases (FeSb and Fe_3O_4) and magnetic diffraction peaks of CuFeSb/minor Fe_3O_4 phase.

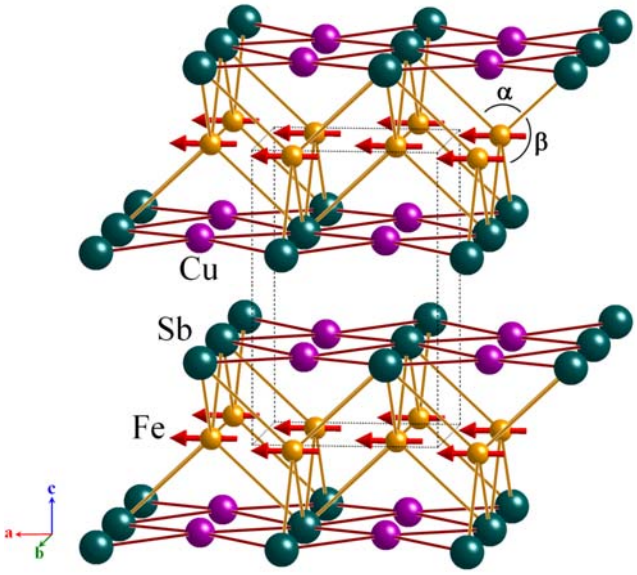

Figure 2 (Color online). Crystal structure of CuFeSb.

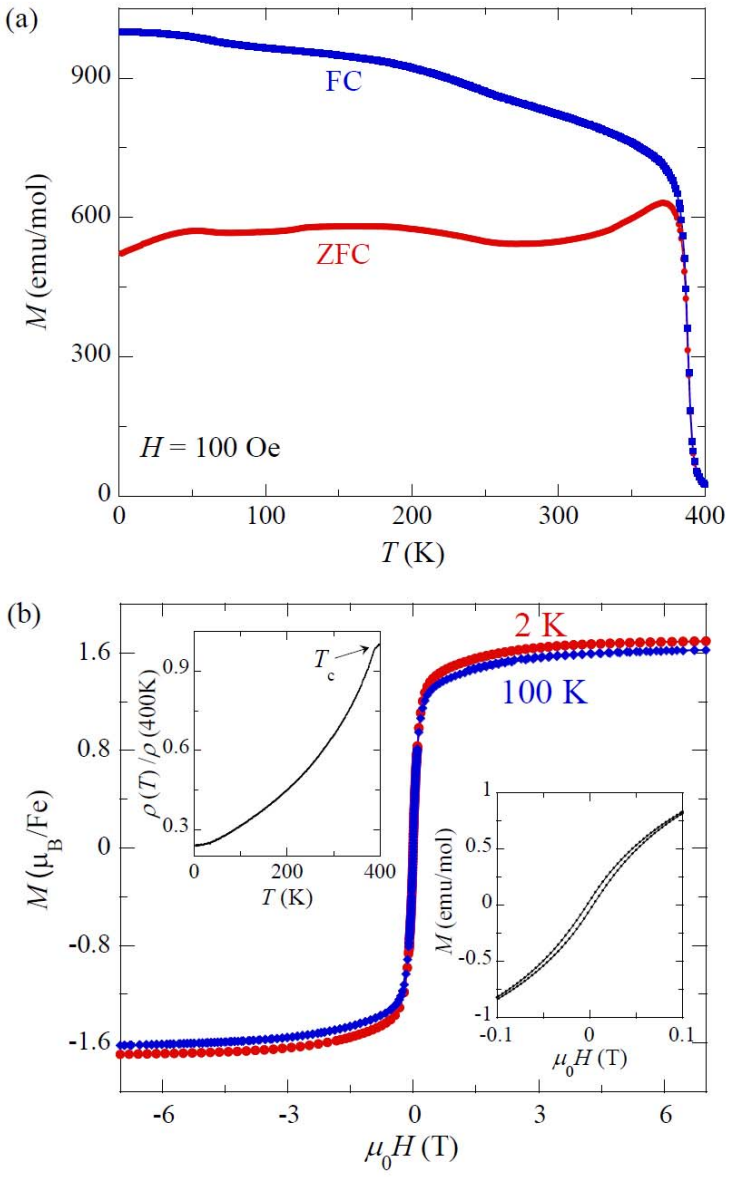

Figure 3 (Color online). (a) Magnetization as a function of temperature $M(T)$ of CuFeSb measured with ZFC and FC histories. (b) Magnetization as a function of magnetic field $M(H)$ of CuFeSb at 2 and 100 K. Left Inset: the temperature dependence of resistivity. Right inset: the magnetic hysteresis loop at 2 K.

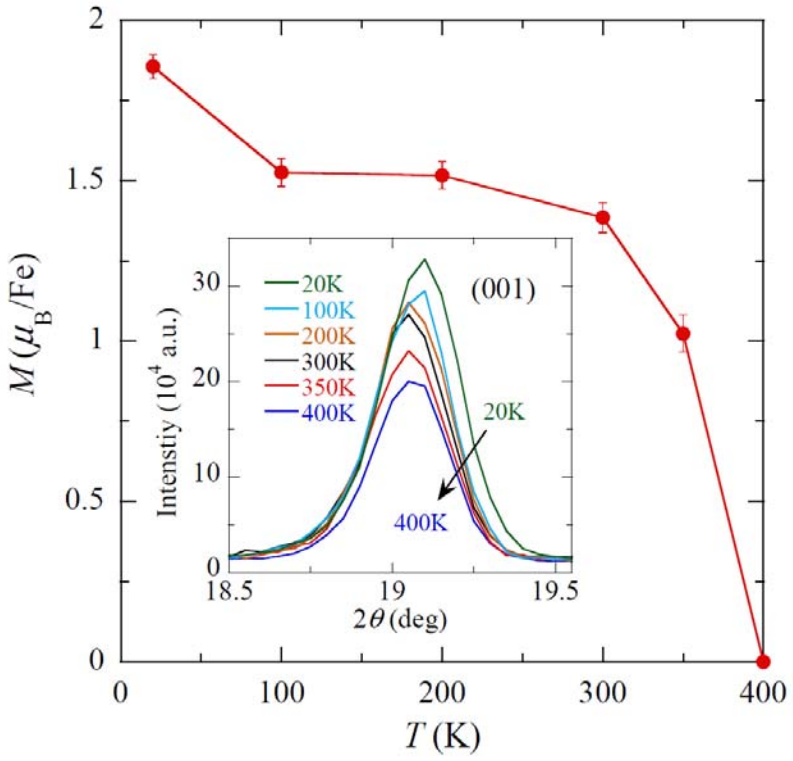

Figure 4 (Color online). The ordered magnetic moment as a function of temperature extracted from the magnetic structure refinements of neutron powder diffraction spectra for CuFeSb. Inset: (001) diffraction peak at various temperatures.